

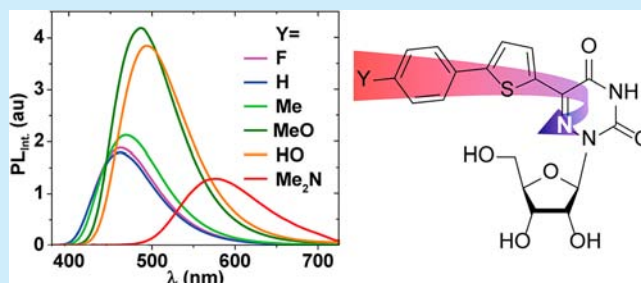
Visibly Emissive and Responsive Extended 6-Aza-Uridines

Patrycja A. Hopkins, Renatus W. Sinkeldam, and Yitzhak Tor*

Department of Chemistry and Biochemistry, University of California, San Diego, 9500 Gilman Drive, La Jolla, California 92093, United States

Supporting Information

ABSTRACT: A family of extended 5-modified-6-aza-uridines was obtained via Suzuki coupling reactions with a common brominated precursor. Extending the conjugated-6-aza-uridines with substituted aryl rings increases the push–pull interactions yielding enhanced bathochromic shifts and solvatochromism compared to the parent nucleosides. For example, the methoxy substituted derivative **1d** displays $\lambda_{\text{max abs}}$ around 375 nm, with visible emission maxima at 486 nm ($\Phi = 0.74$) and 525 nm ($\Phi = 0.02$) in dioxane and water, respectively.



Diverse approaches have been devised for modifying the nonemissive pyrimidine and purine nucleobases in DNA and RNA into fluorescent surrogates.^{1–4} The fundamental challenges result from both structural and electronic dilemmas, where any modification aimed at enhancing the electronic features favoring fluorescence can hamper the WC face and its tautomeric preferences, as well as the hybridization and folding features of the resulting oligomers. This issue is particularly challenging when one aims at shifting the emission bands further into the visible and red spectral domains. Such low energy emission is frequently associated with relatively large chromophores with physical footprints, which are much larger than the native nucleobases.⁵

Nature exploits various mechanisms to tune the photophysics of its small and environmentally sensitive visibly emitting chromophores, such as oxyluciferin^{6–8} and arylidene-imidazolidones (in fluorescent proteins).^{9–11} Strong charge transfer transitions and proton transfer processes in the excited state typically yield low energy emission, which is dependent on the compactness and polarity of the chromophore's environment.^{12–15} Applying these motifs to visibly emitting nucleosides presents additional challenges. In particular, the electron-withdrawing ability of the native nucleobases needs to be augmented to promote effective CT bands. Diverse efforts have resulted in numerous motifs; most, however, either electronically decouple the native pyrimidine or purine from the actual chromophore¹⁶ or significantly alter the native structure resulting in less than favorable hybridization features.^{17–19}

Here we combine several key features to advance a family of visibly emitting pyrimidine analogs. Figure 1 depicts the evolution of our design principles, illustrating the transformation of uridine into visibly emissive nucleosides. Conjugation of a 5-membered heterocycle, such as thiophene, at the 5 position of uridine, a “dark” nonemissive native nucleoside ($\Phi \sim 10^{-4}$), yielded our first-generation fluorescent nucleosides (**A**, Figure 1). Depending on the conjugated heterocycle, such 5-modified

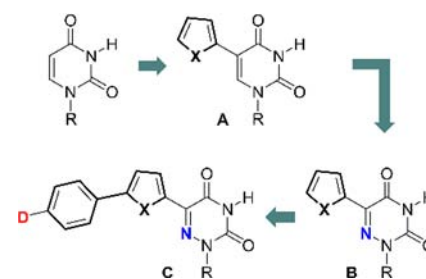


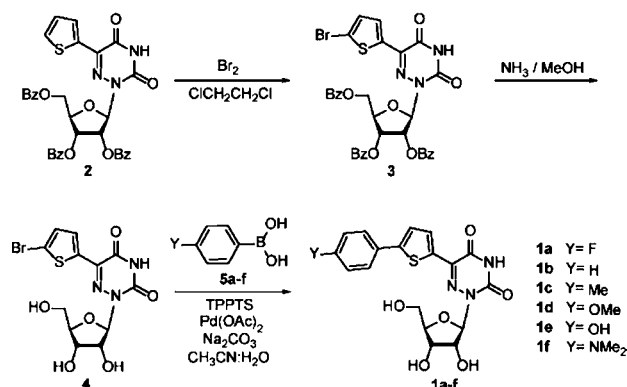
Figure 1. Evolution of the design elements leading to visibly emitting nucleosides.

pyrimidines emit in the visible range (390–443 nm) and have very large Stokes shifts (8400–9700 cm^{-1}), while their quantum efficiency is relatively low ($\Phi = 0.01–0.035$).^{20,21} Further enhancing the polarization of this conjugated electron-poor/electron-rich biaryl system by introducing the electronegative nitrogen at the pyrimidine's 6-position (**B**, Figure 1) resulted in red-shifted absorption and emission maxima and substantially augmented quantum yields ($\Phi = 0.2–0.8$).²² To further shift the emission into the red region of the spectrum, we have advanced the family shown here by directly conjugating a donor group through an extended aromatic system to the electron-deficient 6-aza U (**C**, Figure 1). Here we disclose the synthesis, as well as structural and photophysical features of this advanced visibly emitting motif.

Although multiple synthetic approaches are conceivable, we have selected Suzuki coupling reactions as the key step in constructing all derivatives (**1a–f**) from one common precursor (Scheme 1). Bromination of the protected nucleoside **2**, which was synthesized using a previously published procedure,²² gave **3** in very good yields (Scheme 1, Figure 2a). Deprotection with

Received: August 16, 2014

Published: October 6, 2014

Scheme 1. Syntheses of Nucleosides 1a–f²²

^aSee Supporting Information for synthetic procedures and analytical data.

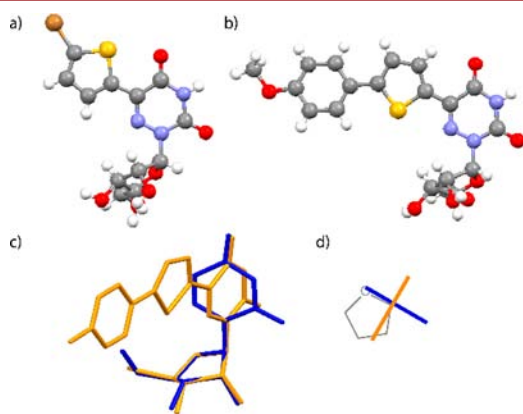


Figure 2. (a, b) X-ray crystal structures of **4** and **1d**, respectively; (c) overlay of X-ray crystal structure of **1c** (orange) with uridine (blue); overlaying the ribose rings shows minimal impact on the sugar pucker (rmsd = 0.04 Å); (d) schematic top view illustrating the relative conformation of the nucleobases in uridine (blue) and **1c** (orange).

methanolic ammonia at 60 °C, followed by recrystallization, yielded **4**. All extended nucleosides **1a–f** were obtained via a Suzuki coupling reaction between **4** and boronic acids **5a–f**,^{23,24} using a combination of a water-soluble ligand, tris(3-sulphophenyl)phosphine trisodium salt (TPPTS), and palladium acetate as a catalyst.²⁵ Trituration with water and recrystallization from methanol afforded pure **1a–f** (49–74%). All nucleosides were thoroughly characterized by ¹H and ¹³C NMR spectroscopy as well as by HRMS and crystallography.²⁵

The crystal structure of **1d** (Figure 2b) illustrates the common structural features of these extended nucleosides (see also Figures S2.2–S2.6). Overlaying the structures of uridine and **1c** (Figure 2c) shows the minimal impact on the sugar pucker, although with a noticeable difference in the dihedral angle χ (−164.41° and −89.0° for uridine and **1c**, respectively; Figure 2d). Such differences are likely a result of crystal packing forces, as the extended derivatives frequently show extensive aromatic–aromatic interactions in the solid state (see Figure S3.1).

To evaluate their basic features and assess the influence of the remote substituents on the photophysical properties of **1a–f**, absorption and emission spectra were recorded in dioxane and water (Figure 3, Table 1). The absorption maxima of all nucleosides are red-shifted compared to the parent conjugated aza-uridine²² and found in the low energy range of the UV spectrum (350–400 nm). All nucleosides **1a–f** are visibly

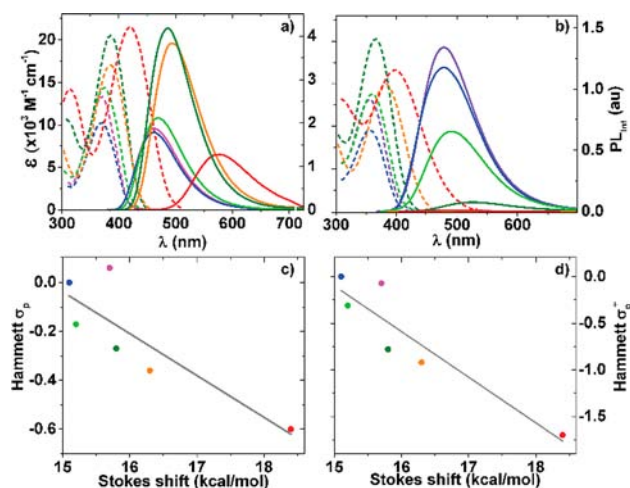


Figure 3. Molar absorptivity (dotted line) and emission (solid line) spectra for **1a** (purple), **1b** (blue), **1c** (green), **1d** (dark green), **1e** (orange), and **1f** (red) in dioxane (a) and water (b). Emission was recorded after excitation at $\lambda_{\text{abs max}}$ for each derivative (Table 1). Calculated Stokes shift in kcal/mol for spectra taken in dioxane are correlated with Hammett σ_{para} (c) and Hammett σ_{para}^+ (d).

fluorescent, covering a wide window of emission energies ranging from ca. 450 to 600 nm. All display rather large Stokes shifts (>5000 cm^{-1}), which for all derivatives but one (**1f**) become even more pronounced as polarity increases (>7000 cm^{-1}). Their emission quantum yields in dioxane are moderate to high (0.2–0.75), but drop in a substitution-dependent manner, as discussed below, when taken in more polar solvents.

Increasing the electron-rich character of the substituent on the phenyl ring results in a bathochromic shift for both absorption and emission maxima in the following general order: **1a** \approx **1b** < **1c** < **1d** < **1e** < **1f**.²⁶ This illustrates the impact of the substituent on both the ground and excited state. In apolar media the highest quantum yield is observed for derivatives with oxygen-containing substituents **1d** and **1e** (0.74 and 0.71, respectively). The opposite is observed in polar protic media where the less electron-rich substitutions show a higher fluorescent intensity while strong fluorescent quenching is observed for the most electron-rich derivatives **1e** and **1f** compared to **1a–d**. Such facilitation of nonradiative decay pathways for fluorophores capable of H-bonding is not uncommon.^{13,27,28} Correlating the calculated Stokes shifts observed in dioxane against Hammett σ_{para} and σ_{para}^+ parameters shows a reliable trend (Figure 3c,d). This provides a useful design tool enabling the use of established linear free energy parameters to confidentially anticipate select photophysical properties.^{29,30}

To evaluate the influence of polarity on the nucleosides' photophysical properties and hence their responsiveness, spectra were measured in dioxane [$E_{\text{T}}(30) = 36.0$ kcal/mol], methanol [$E_{\text{T}}(30) = 55.4$ kcal/mol], and mixtures thereof.³¹ For each solution the $E_{\text{T}}(30)$ value was experimentally determined using Reichardt's dye.³² While absorption spectra show little to no variation as polarity is systematically varied,³³ significant changes are seen in both emission wavelengths and intensity (Figure 4a,b).³⁴ With increasing polarity a bathochromic shift of $\lambda_{\text{em max}}$ was seen for all extended nucleosides **1a–f**. For example, the emission maximum of **1c** is 468 in dioxane and 499 nm in methanol. Similar trends were reported for the parent 5-thiopheno-6-aza-uridine,²² and 5-thiopheno-uridine.³⁵ To better quantify this effect, Stokes shifts were calculated for each sample

Table 1. Photophysical Properties of Nucleosides 1a–f^a

compound	substituent Y	solvent	absorption		emission		brightness $\Phi \times \epsilon \times 10^3$	Stokes shift	
			λ_{\max} [nm]	ϵ^b	λ_{\max} [nm]	Φ^c		$\nu_{\text{abs}} - \nu_{\text{em}}$ [cm ⁻¹]	[kcal/mol]
B ²²	(R = ribose) (X = S)	dioxane	335	13	415	0.80	10.4	6025	16.4
		methanol	334	11	433	0.50	5.5	7332	19.6
		water	332	11	455	0.20	2.2	8492	23.3
1a	F	dioxane	368	15.0	462	0.32	4.8	5504	15.7
		methanol	365	14.0	488	0.11	1.5	6867	19.6
		water	357	12.6	478	0.24	3.0	7140	20.4
1b	H	dioxane	371	9.7	461	0.30	2.9	5286	15.1
		methanol	367	8.9	488	0.16	1.4	6767	19.3
		water	356	9.6	478	0.21	2.0	7184	20.5
1c	Me	dioxane	375	14.6	468	0.38	5.6	5308	15.2
		methanol	372	14.0	499	0.07	1.0	6855	19.6
		water	360	13.9	490	0.12	1.7	7370	21.1
1d	MeO	dioxane	383	20.8	486	0.74	15.4	5534	15.8
		water	366	19.7	525	0.02	0.4	8275	23.7
1e	HO	dioxane	385	16.9	494	0.71	12.0	5695	16.3
		water	381	15.0	517	<0.01	<0.1	6944	19.8
1f	Me ₂ N	dioxane	420	21.4	575	0.20	4.3	6428	18.4
		water	398	16.8	484	<0.01	<0.1	4464	12.8

^aAbsorption and steady-state emission spectroscopy studies were performed using samples prepared from a concentrated DMSO stock solution.²⁵ ^b ϵ in [$\times 10^3 \text{ M}^{-1} \text{ cm}^{-1}$]. ^cFluorescence standards: Coumarin 102 was used for 1a–e, and Coumarin 153 was used for 1f.

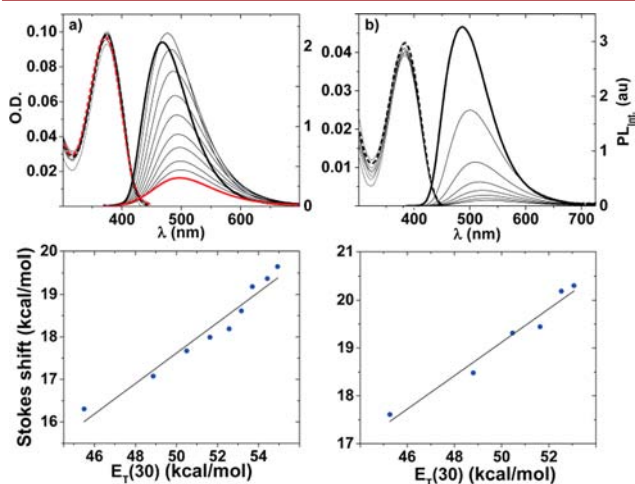


Figure 4. (a,b) Assessing the effect of solvent polarity on absorption (dotted line) and emission (solid line), in dioxane (bold black line), methanol (bold red line), and their mixtures (black lines) for 1c ($6.7 \times 10^{-6} \text{ M}$) and 1d ($2.0 \times 10^{-6} \text{ M}$); respectively.²⁵ (c, d) Correlating Stokes shift vs $E_T(30)$ values obtained from dioxane–methanol mixtures for 1c (90%:10% \rightarrow 10%:90%; slope: 0.36 and $R^2 = 0.95$) and 1d (90%:10% \rightarrow 40%:60%; slope: 0.35 and $R^2 = 0.98$).²⁵ Experimental errors are smaller than the data symbols; see SI for enlarged correlations (Figures S8.1 and S8.2).

containing the dioxane/methanol mixture and plotted against the experimentally determined $E_T(30)$ values. As with related emissive nucleosides, a linear fit is observed (Figure 4c,d). Additionally, a steady decrease in the integrated emission was observed for 1c and 1d (as well as the parent 5-thiopheno-6-aza-uridine,²² and 5-thiophene-uridine³⁵) as the content of the protic solvent (e.g., H₂O, MeOH) increases. This phenomenon is rather common in fluorophores that display significant charge transfer character in their excited state.^{13,36}

In summary, visibly emitting, bright, and responsive nucleosides have been obtained by implementing an enhanced charge transfer character in 5-substituted 6-aza-uridines. The photophysical features of these synthetically accessible analogs can be tuned by judiciously introducing substituents of distinct electronic character at a remote but conjugated position. In general, the extended analogs reported here display higher emission quantum yields in apolar solvents but remain sufficiently bright in polar media. This trend is, however, dependent on the nature of the substituent with highly electron-rich derivatives suffering the highest loss in emission quantum yield. Nevertheless, the highly desirable and tunable photophysical properties, including pronounced solvatochromism, make this 6-aza-uridine motif a very attractive scaffold for the design and development of useful biophysical probes.

■ ASSOCIATED CONTENT

Supporting Information

Experimental procedures and full characterization details including, ¹H, ¹³C, and ¹⁹F NMR, as well as crystal structures. This material is available free of charge via the Internet at <http://pubs.acs.org>.

■ AUTHOR INFORMATION

Corresponding Author

*E-mail: ytor@ucsd.edu.

Notes

The authors declare no competing financial interest.

■ ACKNOWLEDGMENTS

This work was supported by a grant from the NIH (GM 069773). We are grateful to Drs. Curtis Moore and Arnold Rheingold (UCSD Chemistry and Biochemistry X-ray Facility) for their help.

■ REFERENCES

- (1) Sinkeldam, R. W.; Greco, N. J.; Tor, Y. *Chem. Rev.* **2010**, *110*, 2579.
- (2) Wilhelmsson, L. M. *Q. Rev. Biophys.* **2010**, *43*, 159.
- (3) (a) Hawkins, M. E. *Cell Biochem. Biophys.* **2001**, *34*, 257. (b) Okamoto, A.; Saito, Y.; Saito, I. *J. Photochem. Photobiol., C* **2005**, *6*, 108. (c) Dodd, D. W.; Hudson, R. H. E. *Mini-Rev. Org. Chem.* **2009**, *6*, 378.
- (4) (a) Rist, M. J.; Marino, J. P. *Curr. Org. Chem.* **2002**, *6*, 775. (b) Wilson, J. N.; Kool, E. T. *Org. Biomol. Chem.* **2006**, *4*, 4265. (c) Kimoto, M.; Cox, R. S., III; Hirao, I. *Expert Rev. Mol. Diagn.* **2011**, *11*, 321.
- (5) Lavis, L. D.; Raines, R. T. *ACS Chem. Biol.* **2008**, *3*, 142.
- (6) Wood, K. V.; Lam, Y. A.; Seliger, H. H.; Mcelroy, W. D. *Science* **1989**, *244*, 700.
- (7) Branchini, B. R.; Magyar, R. A.; Murtiashaw, M. H.; Anderson, S. M.; Helgerson, L. C.; Zimmer, M. *Biochemistry* **1999**, *38*, 13223.
- (8) Branchini, B. R.; Southworth, T. L.; Murtiashaw, M. H.; Magyar, R. A.; Gonzalez, S. A.; Ruggiero, M. C.; Stroh, J. G. *Biochemistry* **2004**, *43*, 7255.
- (9) Tsien, R. Y. *Annu. Rev. Biochem.* **1998**, *67*, 509.
- (10) (a) Wachter, R. M. *Acc. Chem. Res.* **2007**, *40*, 120. (b) Tolbert, L. M.; Baldrige, A.; Kowalok, J.; Solntsev, K. M. *Acc. Chem. Res.* **2012**, *45*, 171.
- (11) Wachter, R. M. *Photochem. Photobiol.* **2006**, *82*, 339.
- (12) Nakatsu, T.; Ichiyama, S.; Hiratake, J.; Saldanha, A.; Kobashi, N.; Sakata, K.; Kato, H. *Nature* **2006**, *440*, 372.
- (13) (a) Strong donor/acceptor interactions are also found in synthetic fluorophores such as PRODAN and cyanine dyes. See: Lakowicz, J. R. *Principles of fluorescence spectroscopy*, 3rd ed.; Springer: New York, 2006.
- (14) Raymond, S. B.; Skoch, J.; Hills, I. D.; Nesterov, E. E.; Swager, T. M.; Bacskaï, B. J. *Eur. J. Nucl. Med. Mol. Imaging* **2008**, *35* (Suppl 1), S93.
- (15) Meek, S. T.; Nesterov, E. E.; Swager, T. M. *Org. Lett.* **2008**, *10*, 2991.
- (16) Riedl, J.; Menova, P.; Pohl, R.; Orsag, P.; Fojta, M.; Hocek, M. *J. Org. Chem.* **2012**, *77*, 8287.
- (17) Gaballah, S. T.; Collier, G.; Netzel, T. L. *J. Phys. Chem. B* **2005**, *109*, 12175.
- (18) Grunwald, C.; Kwon, T.; Piton, N.; Forster, U.; Wachtveitl, J.; Engels, J. W. *Bioorg. Med. Chem.* **2008**, *16*, 19.
- (19) Okamoto, A.; Tainaka, K.; Fujiwara, Y. *J. Org. Chem.* **2006**, *71*, 3592.
- (20) Greco, N. J.; Tor, Y. *J. Am. Chem. Soc.* **2005**, *127*, 10784.
- (21) (a) Greco, N. J.; Tor, Y. *Tetrahedron* **2007**, *63*, 3515. (b) Sinkeldam, R. W.; Wheat, A. J.; Boyaci, H.; Tor, Y. *ChemPhysChem* **2011**, *12*, 567.
- (22) Sinkeldam, R. W.; Hopkins, P. A.; Tor, Y. *ChemPhysChem* **2012**, *13*, 3350.
- (23) Kovaliov, M.; Segal, M.; Fischer, B. *Tetrahedron* **2013**, *69*, 3698.
- (24) Capek, P.; Pohl, R.; Hocek, M. *Org. Biomol. Chem.* **2006**, *4*, 2278.
- (25) See Supporting Information for additional details.
- (26) This is true for nucleosides **1a–f**, with the exception of **1e** and **1f** when taken in water.
- (27) Zhao, G. J.; Han, K. L. *Acc. Chem. Res.* **2012**, *45*, 404.
- (28) Liu, Y. H.; Zhao, G. J.; Li, G. Y.; Han, K. L. *J. Photochem. Photobiol., A* **2010**, *209*, 181.
- (29) (a) Tzalis, D.; Tor, Y. *Tetrahedron Lett.* **1995**, *36*, 6017. (b) Joshi, H. S.; Jamshidi, R.; Tor, Y. *Angew. Chem., Int. Ed.* **1999**, *38*, 2722.
- (30) (a) Mizuta, M.; Seio, K.; Ohkubo, A.; Sekine, M. *J. Phys. Chem. B* **2009**, *113*, 9562. (b) Wahba, A. S.; Azizi, F.; Deleavey, G. F.; Brown, C.; Robert, F.; Carrier, M.; Kalota, A.; Gewirtz, A. M.; Pelletier, J.; Hudson, R. H. E.; Damha, M. J. *ACS Chem. Biol.* **2011**, *6*, 912. (c) Kovaliov, M.; Weitman, M.; Major, D. T.; Fischer, B. *J. Org. Chem.* **2014**, *79*, 7051.
- (31) As apparent from their structures, the photophysical features of the azauridine-based nucleosides are inherently sensitive to changes in pH. Ionizable groups (e.g., OH) further complicate their acid/base features. Titration of **1c** between pH 2 and 12, however, gives a single pK_a value of 6.7 (Figure S7.1, S7.2), similar to the value obtained for the unmodified parent system (ref 22).
- (32) Reichardt, C. *Chem. Rev.* **1994**, *94*, 2319.
- (33) This statement is true for methanol, dioxane, and their mixtures. When comparing the differences between absorption maxima in dioxane and water, however, the shifts are more significant.
- (34) Although low quantum yield values were observed for **1e** and **1f** in water, it is important to note that all modified nucleosides besides **1b** have higher extinction coefficients compared to the parent compound **B**.
- (35) Srivatsan, S. G.; Tor, Y. *Chem.—Asian J.* **2009**, *4*, 419.
- (36) Dhuguru, J.; Liu, W. J.; Gonzalez, W. G.; Babinchak, W. M.; Miksovská, J.; Landgraf, R.; Wilson, J. N. *J. Org. Chem.* **2014**, *79*, 4940.